

Quasinormal modes of Schwarzschild Black Hole and Damour-Solodukhin Wormhole via Feedforward Neural Network Method

Ali Övgün,^{1,2,*} İzzet Sakallı,^{2,†} and Halil Mutuk^{3,‡}

¹*Instituto de Física, Pontificia Universidad Católica de Valparaíso, Casilla 4950, Valparaíso, Chile.*

²*Physics Department, Faculty of Arts and Sciences,
Eastern Mediterranean University, Famagusta, North Cyprus, via Mersin 10, Turkey.*

³*Physics Department, Faculty of Arts and Sciences,
Ondokuz Mayıs University, 55139, Samsun, Turkey.*

(Dated: December 20, 2024)

For the first time in the literature, we show how the quasinormal modes (QNMs) arising from the perturbations of scalar fields propagating in the backgrounds of a black hole and wormhole can be derived by using the feedforward neural network method (FNNM). To this end, as examples, we consider the QNMs of Schwarzschild black hole and Damour-Solodukhin wormhole. It is shown that the obtained QNMs via the FNNM are in good agreement with the former results obtained from the other well-known numerical methods. Our analysis can then be generalized to the other black holes having more than one horizon and even to more exotic black hole/wormhole geometries.

Keywords: Quasinormal modes; Feedforward Neural network; Wormhole; Black hole

I. INTRODUCTION

QNMs are complex frequency modes that rule the time evolution of perturbations of systems which contingent on damping either by internal dissipation or by radiating away energy. Imaginary part of the complex number of a QNM is inversely proportional to the damping time. On the other hand, the damping can occur even without friction, since the energy could be faded away towards infinity by gravitational waves according to the general relativity (GR) theory. QNMs of black hole have been investigated for a long time and much have been known in various cases (see for example [1–24]). Similar to the black hole geometries, a wormhole spacetime is also an open system in which QNMs appear too [25–34]. Namely, the fields entering into an irreversible wormhole can also be detected with the QNMs having dissipating energy and decay.

It is worth noting that in 1916 (a few months after Schwarzschild published his solution), the first time in history, Flamm suggested that wormholes are theoretically possible. Besides, he also defined the white holes that throw everything out, which has opposite features of the black holes. An explicit example of a wormhole metric was investigated by Einstein and Rosen in their 1935 paper [35] and came to be known as the Einstein-Rosen bridge. The Einstein-Rosen bridge is a shortcut that could reduce the distance and travel time. In 1957, the term wormhole was first coined by Misner and Wheeler [36] and their conceptual study addresses a quick interstellar travel without neglecting the universal speed limit

c. Even the science fiction books and movies were inspired by their work: by producing a suitable spacecraft, a quick interstellar journey would be possible without ignoring the universal speed limit *c*. On the other hand, scientific interest in the possibility of traversable wormholes did not occur until 1985 [37]. In writing his novel “Contact”, Carl Sagan consulted physicists Thorne and Morris to get help for illustrating a convincing wormhole, and Thorne and Morris found a rather simple example of a remarkably traversable wormhole that is almost entirely compatible with GR [38, 39]. To this end, they started with the assumption of having spherical symmetry and asymptotically two flat regions coherent with the Einstein-Rosen bridge (as being discussed above). In the sequel, they managed to construct a traversable wormhole metric that enables the geodesics to pass from one region to another in a reasonable timescale. Although the wormholes have no event horizon and singularity, it turns out that traversable wormholes are possible under the laws of GR if one allows the so-called exotic matter possessing negative energy to hold the throat of the wormhole open. Then the wormhole idea was further enhanced by numerous studies (see for example [40–42]). On the other hand, the existence of wormholes has not yet been observed. But there are many ideas on how to detect them by using the gravitational waves, QNMs, and gravitational lensing (see for instance [43–63] and references therein). However, today there are promising spectacular observations that encourage us about the future observation of the wormholes. In particular, for the first time ever, mankind has succeeded to photograph one of the black holes: Event Horizon Telescope (EHT), a planet-scale array of eight ground-based radio telescopes forged through international collaboration, has captured the shadow of the supermassive black hole in the center of the galaxy M87. EHT’s results also mesh well with those of the Laser Interferometer Gravitational-Wave Observatory (LIGO), which has detected the spacetime ripples

*Electronic address: ali.ovgun@emu.edu.tr; Electronic address: ali.ovgun@pucv.cl

†Electronic address: izzet.sakalli@emu.edu.tr

‡Electronic address: halilmutuk@gmail.com

generated by mergers involving black holes just a few dozen times more massive than the Sun [64]. Moreover, having the QNMs of a wormhole with enough precision, we can get information about the shape of the wormhole and how fast they can decay [65].

New derivations of the QNMs for black holes and wormholes have always attracted a great attention. This challenge stems from the fact that it is not easy to solve the wave equations of the considered fields, analytically. Therefore, many numerical techniques have been developed in order to solve those type of equations. In recent decades, artificial neural networks (ANNs) [66] are being used for solving the differential equations appeared in the different physical systems. As it is well known, ANN or connectionist systems compute the systems vaguely inspired by the biological neural networks that constitute animal brains. Some of the advantages of using ANNs in solving the differential equations are listed below [67–70]:

- The solution is continuous over all the domain of integration [71],
- Computational complexity does not increase significantly with the number of sampling points and dimensions of the problem,
- Rounding-off error propagation of standard numerical methods does not influence the neural network solution,
- The method requires less number of model parameters and therefore does not ask for high memory space in computer.

In this paper, we mainly focus on the two spacetime geometries in order to show that QNM computations are eligible within the framework of FNNM. The considered spacetimes are Schwarzschild black hole and Damour-Solodukhin wormhole (DSW).

The paper is organized as follows. In Section II, we briefly review the DSW, which is nothing but the Schwarzschild-like wormhole solution. Section III is devoted to the review of the Mashhoon method that uses the Pöschl-Teller potential and it is known as one of the vindicated numerical methods to compute the QNMs [33, 72]. In Section IV, we solve the QNMs numerically by using the FNNM. Then, we present and compare our results with the ones [22, 33] in the literature. Finally, we discuss our results and conclude in section V. We follow the metric convention $(-, +, +, +)$.

II. DSW SPACETIME

In this section, we make a brief overview of the DSW [44], which is described by the following metric:

$$ds^2 = -(1 - 2M/r + \lambda^2)dt^2 + \frac{dr^2}{1 - 2M/r} + r^2 d\Omega_{(2)}^2. \quad (2.1)$$

As can be seen from above, when the parameter $\lambda = 0$, the DSW becomes Schwarzschild black hole. When λ^2 is different than zero, the Einstein tensor of (2.1); G_{tt} is zero, but $G_{rr}, G_{\theta\theta}, G_{\phi\phi} \sim \lambda^2$ which means that it requires some matter.

It is important to note that the metric in (2.1) can be rewritten by using $t \rightarrow t/\sqrt{1 + \lambda^2}$ and $M \rightarrow M(1 + \lambda^2)$:

$$ds^2 = -A(r)dt^2 + \frac{dr^2}{B(r)} + r^2 d\Omega_{(2)}^2, \quad (2.2)$$

where

$$A(r) = 1 - \frac{2M}{r}, \quad B(r) = 1 - \frac{r_h}{r}, \quad (2.3)$$

where $r_h = 2M(1 + \lambda^2)$ denotes the horizon.

In the next sections, we shall briefly review one of the well-known numerical methods – Mashhoon method – to show how one can compute the numerical QNMs of Schwarzschild black hole and DSW. Then, first time in literature, we are going to study QNMs of Schwarzschild black hole and DSW by employing the FNNM.

III. QNMS VIA MASHHOON METHOD

To compute the QNMs of black holes and wormholes via the Mashhoon method [72], we first consider the massless Klein-Gordon equation (KGE) which is given by

$$\nabla^2 \Phi = 0, \quad (3.1)$$

and use the following scalar field ansatz (due to the spherically symmetric structure spherical harmonics modes):

$$\Phi(r, \theta, \phi, t) = \frac{\Psi(r)}{r} Y_{lm}(\theta, \phi) e^{-i\omega t}. \quad (3.2)$$

We note that ω is the oscillating frequency of the scalar field, l stands for the angular quantum number and m is for the magnetic quantum number. Afterwards, the KGE is separated into the following form:

$$\Psi''(r) + (\omega^2 - V_0(r)) \Psi(r) = 0, \quad (3.3)$$

where the effective potential reads

$$V_0(r) = \frac{l(l+1)f(r)}{r^2} + \frac{[f(r)g(r)]'}{2r}. \quad (3.4)$$

Here, a prime symbol stands for the derivative with respect to the tortoise coordinates (r_*) , $dr_* = \frac{dr}{f(r)}$. Since the QNM is a bound-state problem with a potential $V_0 \rightarrow -V_0$, the wave functions become zero at the boundaries. Furthermore, we use the Pöschl-Teller potential [33, 72]:

$$V_{PT} = \frac{V_{0max}}{\cosh^2 \alpha(r_* - r)} \quad (3.5)$$

to model the dynamics of fields propagating around black holes or wormholes. In Eq. (3.5), $V_{0_{max}}$ is the value of the effective potential (3.4) at the maximum point. The bound states of the Pöschl-Teller potential are governed by

$$\omega(\alpha) = W(\alpha'), \quad (3.6)$$

where

$$W(\alpha') = \alpha' \left[-\left(n + \frac{1}{2}\right) + \frac{1}{4} + \sqrt{\frac{V_{0_{max}}}{\alpha'^2}} \right]. \quad (3.7)$$

Using the inverse bound states (i.e., $\alpha' = i\alpha$), one can obtain the QNM frequencies (ω) as follows

$$\omega = \pm \sqrt{V_{0_{max}} - \frac{1}{4}\alpha^2 - i\alpha\left(n + \frac{1}{2}\right)}, \quad (3.8)$$

in which n represents the overtone quantum numbers.

IV. QNM COMPUTATIONS VIA FNNM

Nowadays, ANN is one of the popular topics of machine learning paradigm. They have a wide range of usage from pattern recognition to financial forecast including classification, decoding speech etc. ANNs are typically composed of layers. These layers are made of interconnected neurons (perceptrons in computerized systems). A neuron is the basic processing element in the ANN. Because, neurons have activation functions which translate input signals to output signals. Problem solving process in the ANN occurs by acquiring knowledge. This mechanism is maintained by learning methods and information is stored within 'interneuron connections' strength which can be calculated by some numerical values called weights [73].

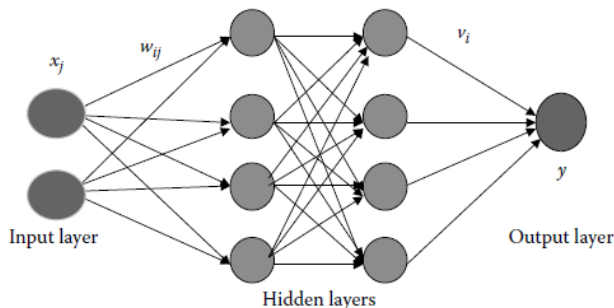


FIG. 1: A sample architecture of an artificial neural network.

A schematic diagram of a multilayer neural network is given in Fig. (1). The information are given to the input layer, which sends the information to the hidden layer, if any exists. The processing of inputs are being done

at this stage via a system of weighted connections. The hidden layers send the information to the output layer and an answer is given to the outside world. In Fig. (1), x_j are input nodes, w_{ij} are weights from input layers to the hidden layer(s), and ν_i are the weights from hidden layer(s) to the output layer y that is the output node [73]. There is no connection among the neurons located in the same layer.

The mathematical formulation of the ANN can be seen in Fig. (2).

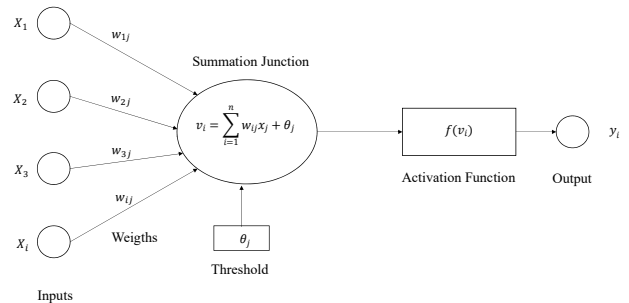


FIG. 2: Mathematical deconstruction of ANN

A neuron (perceptron in computerized systems) N_i accepts a set of n inputs which is an element of the set $S = \{x_j | j = 1, 2, \dots, n\}$. Each input is weighted before entrance of a neuron N_i by weight factor w_{ij} for $j = 1, 2, \dots, n$. Furthermore, it has bias term w_0 , a threshold value θ_k which has to be reached or exceeded for the neuron to produce output signal. Mathematically, the output of the i -th neuron N_i is given by

$$O_i = f\left(w_0 + \sum_{j=1}^n w_{ij}x_j\right). \quad (4.1)$$

The neuron's *work* condition is defined as

$$w_0 + \sum_{j=1}^n w_{ij}x_j \geq \theta, \quad (4.2)$$

and the input signal of the i -th neuron N_i is given by

$$v_i = w_0 + \sum_{j=1}^n w_{ij}x_j. \quad (4.3)$$

A function $f(s)$ acts on the produced weighted signal. This function is called activation function. The output signal obtained by activation function reads

$$O_i = f(v_i - \theta_i). \quad (4.4)$$

All inputs are multiplied by their weights and added together to form the net input to the neuron. This is called *net* and can be written as

$$\text{net} = \sum_{j=1}^n w_{ij}x_j + \theta, \quad (4.5)$$

where θ is a threshold value which is added to the neuron. The neuron takes these inputs and produce an output y by mapping function $f(\text{net})$

$$y = f(\text{net}) = f\left(\sum_{j=1}^n w_{ij}x_j + \theta\right) \quad (4.6)$$

where f is the neuron activation function. Generally the neuron output function is proposed with a threshold function, which can be one of the linear, sign, sigmoid or step functions. In this study, we shall consider a sigmoid activation function:

$$f(x) = \frac{1}{1 + e^{-x}} \quad (4.7)$$

which is typical in multilayer perceptron neural networks.

A. Implementation of ANN on Quantum Systems

In this part, we will follow the formalism for FNNM which was developed in Ref. [74]. Any differential equation can be written in the following form:

$$H\Psi(r) = f(r), \quad (4.8)$$

where H is a linear operator, $f(r)$ is an arbitrary function, and $\Psi(r)$ should vanish at the boundaries. For solving Eq. (4.8), one may consider the following trial function:

$$\Psi_t(\mathbf{r}) = C(\mathbf{r}) + D(\mathbf{r}, \Lambda)N(\mathbf{r}, \mathbf{p}), \quad (4.9)$$

which proceeds to a neural network with a vector parameter vector \mathbf{p} and undetermined parameter Λ which is going to be adjusted later. In fact, \mathbf{p} corresponds to the weights and biases of the neural architecture. $C(\mathbf{r})$ and $D(\mathbf{r}, \Lambda)$ are determined in such a way that $\Psi_t(\mathbf{r})$ satisfies the boundary conditions regardless of \mathbf{p} and Λ values. In order to solve Eq. (4.8), the collocation method [75] can be used. To this end, one can get a minimization problem as follows:

$$\min_{p, \Lambda} \sum_i [H\Psi_t(r_i) - f(r_i)]^2. \quad (4.10)$$

To have the Schrödinger equation, one can recast Eq. (4.8) in an eigenvalue equation:

$$H\Psi(r) = \omega^2\Psi(r) \quad (4.11)$$

with the boundary condition $\Psi(r = 0) = 0$. Here, it is worth noting that we shall follow the foreknown definition of the QNMs that these modes are purely outgoing waves at the horizon r_h and vanish at $r = 0$ [76]. Indeed these boundary conditions are determined by the behavior of the effective potential Eq. (3.4). Thus, the trial solution becomes

$$\Psi_t(r) = D(\mathbf{r}, \Lambda)N(\mathbf{r}, \mathbf{p}) \quad (4.12)$$

where $D(\mathbf{r}, \Lambda) = 0$ at boundary conditions for a range of Λ values. By discretizing the domain of the problem, a minimization problem can be obtained with respect to the parameters \mathbf{p} and Λ :

$$E(\mathbf{p}, \Lambda) = \frac{\sum_i [H\Psi_t(r_i, \mathbf{p}, \Lambda) - \omega^2\Psi_t(r_i, \mathbf{p}, \Lambda)]^2}{\int |\Psi_t|^2 d\mathbf{r}}, \quad (4.13)$$

where E is the error function. Furthermore, ω^2 can be obtained as follows

$$\omega^2 = \frac{\int \Psi_t^* H\Psi_t d\mathbf{r}}{\int |\Psi_t|^2 d\mathbf{r}}. \quad (4.14)$$

Thus, the energy eigenvalues or the QNMs are given by

$$\omega = \left(\frac{1}{\int |\Psi_t|^2 d\mathbf{r}} \left[\int_0^{r_h} \left(\frac{d\Psi_t}{dr} \right)^2 dr + \int_0^{r_h} V_0(r)\Psi_t^2(r)dr \right] \right)^{\frac{1}{2}}. \quad (4.15)$$

In this study, we consider a multilayer perceptron with n input units, one hidden layer with m units, and one output. For a given input vector

$$\mathbf{r} = (r_1, \dots, r_n), \quad (4.16)$$

the output of the network can be written as

$$N = \sum_{i=1}^m \nu_i \sigma(z_i), \quad (4.17)$$

where

$$z_i = \sum_{j=1}^n \gamma_{ij}r_j + u_i. \quad (4.18)$$

Here, γ_{ij} refers the weight from input unit j to the hidden unit i , ν_i is the weight from hidden unit i to the output, u_i represents the bias of hidden unit i , and $\sigma(z)$ is the sigmoid function, which is given in Eq. (4.7). The network output derivatives can be defined as

$$\frac{\partial^k N}{\partial r_j^k} = \sum_{i=1}^m \nu_i \gamma_{ij}^k \sigma_i^{(k)}, \quad (4.19)$$

where $\sigma_i = \sigma(z_i)$ and $\sigma^{(k)}$ is the k^{th} order derivative of the sigmoid function.

One can parametrize the trial function as

$$\phi_t(r) = e^{-\beta r^2} N(r, \mathbf{u}, \mathbf{w}, \mathbf{v}), \quad \beta > 0 \quad (4.20)$$

where N denotes a feedforward ANN with one hidden layer and \bar{m} sigmoid hidden units

$$N(r, \mathbf{u}, \mathbf{w}, \mathbf{v}) = \sum_{j=1}^{\bar{m}} \nu_j \sigma(\omega_j r + u_j). \quad (4.21)$$

The minimization problem turns out to be as

$$\frac{\sum_i [H\phi_t(r_i) - \omega^2 \phi_t(r_i)]^2}{\int |\phi_t(r)|^2 dr}. \quad (4.22)$$

Using Eqs. (2.3), (3.3), and (3.4) in Eq. (4.15), we obtain

the QNMs: the integrals seen in Eq. (4.15) have been computed with the Gauss-Legendre rule [74] and we have used 200 equidistant points in the interval $0 < r < 10$ with $\bar{m} = 10$. In Tables I and II, we present the QNMs of the DSW for the $\lambda = 10^{-5}$. Table III and IV illustrate the QNMs of the Schwarzschild black hole (when $\lambda = 0$). It can be seen from those Tables that FNNM satisfactorily re-derives the well-accepted QNMs' results obtained from the other numerical methods [22, 33]. Thus, we believe that we have managed to introduce a new and effective method to the literature as being an alternative to the existing numerical methods.

TABLE I: Comparison of QNMs of DSW for $l = 0, M = 1$ case

Mode n	ω_n [(FNNM) Eq. (4.15)]	ω_n [Pöschl-Teller Eq. (3.8)]	ω_n [(Numerical) [33]]
1	$0.032447 - 1.036376 \times 10^{-5}i$	$0.03230 - 1.666 \times 10^{-4}i$	$0.03210 - 1.083 \times 10^{-4}i$
2	$0.063914 - 6.6689 \times 10^{-5}i$	$0.06427 - 7.413 \times 10^{-4}i$	$0.06382 - 5.720 \times 10^{-4}i$
3	$0.095259 - 1.218 \times 10^{-4}i$	$0.09576 - 1.919 \times 10^{-3}i$	$0.09503 - 1.679 \times 10^{-3}i$
4	$0.126835 - 3.7917 \times 10^{-3}i$	$0.1268 - 3.910 \times 10^{-3}i$	$0.1258 - 3.709 \times 10^{-3}i$
5	$0.156686 - 5.154 \times 10^{-3}i$	$0.1578 - 6.787 \times 10^{-3}i$	$0.1566 - 6.739 \times 10^{-3}i$
6	$0.187675 - 0.01053i$	$0.1888 - 0.01042i$	$0.1877 - 0.01057i$
7	$0.220200 - 0.014978i$	$0.22010 - 0.01456i$	$0.2192 - 0.01490i$
8	$0.251135 - 0.01905i$	$0.2517 - 0.01898i$	$0.2510 - 0.01948i$
9	$0.283984 - 0.023998i$	$0.2835 - 0.02355i$	$0.2832 - 0.02418i$
10	$0.315255 - 0.0291692i$	$0.3155 - 0.02818i$	$0.3158 - 0.02900i$

TABLE II: Comparison of QNMs of DSW for $l = M = 1$ case

Mode n	ω_n [(FNNM) Eq. (4.15)]	ω_n [(Pöschl-Teller) Eq. (3.8)]	ω_n [(Numerical) [33]]
1	$0.0360309 - 5.8173 \times 10^{-7}i$	$0.03616 - 7.280 \times 10^{-7}i$	$0.03501 - 1.962 \times 10^{-8}i$
2	$0.069113 - 4.577302 \times 10^{-6}i$	$0.07196 - 3.831 \times 10^{-6}i$	$0.06982 - 4.390 \times 10^{-7}i$
3	$0.1048921 - 1.658326 \times 10^{-5}i$	$0.1071 - 1.309 \times 10^{-5}i$	$0.1043 - 3.304 \times 10^{-6}i$
4	$0.140620 - 1.397936 \times 10^{-5}i$	$0.1415 - 3.911 \times 10^{-5}i$	$0.1382 - 1.618 \times 10^{-5}i$
5	$0.173859 - 2.14283 \times 10^{-5}i$	$0.1751 - 1.095 \times 10^{-4}i$	$0.1715 - 6.266 \times 10^{-5}i$
6	$0.204056 - 2.802689 \times 10^{-4}i$	$0.2077 - 2.908 \times 10^{-4}i$	$0.2041 - 2.072 \times 10^{-4}i$
7	$0.235528 - 1.06573 \times 10^{-4}i$	$0.2394 - 7.256 \times 10^{-4}i$	$0.2358 - 5.999 \times 10^{-4}i$
8	$0.264457 - 1.306561 \times 10^{-3}i$	$0.2701 - 1.662 \times 10^{-3}i$	$0.2666 - 1.515 \times 10^{-3}i$
9	$0.295845 - 3.6874 \times 10^{-3}i$	$0.3000 - 3.405 \times 10^{-3}i$	$0.2968 - 3.295 \times 10^{-3}i$
10	$0.328118 - 2.27665 \times 10^{-3}i$	$0.3295 - 6.145 \times 10^{-3}i$	$0.3267 - 6.16710^{-3}i$

TABLE III: Comparison of QNMs of Schwarzschild black hole for $n = 0$ and $n = M = 1$ cases

l	QNMs via FNNM $\omega(n = 0)$	$\omega(n = 0)$ [22]	QNMs via FNNM $\omega(n = 1)$	$\omega(n = 1)$ [22]
1	$0.246057 - 0.093018i$	$0.24639 - 0.09322i$	$0.236207 - 0.295596i$	$0.23615 - 0.29639i$
2	$0.459532 - 0.096075i$	$0.45713 - 0.09507i$	$0.435274 - 0.293645i$	$0.43583 - 0.29097i$
3	$0.655795 - 0.096172i$	$0.65673 - 0.09563i$	$0.639540 - 0.290758i$	$0.64147 - 0.28980i$
4	$0.859058 - 0.096771i$	$0.85301 - 0.09587i$	$0.843526 - 0.283506i$	$0.84114 - 0.28934i$
5	$1.041541 - 0.096852i$	$1.04787 - 0.09598i$	$1.038379 - 0.281969i$	$1.03815 - 0.28911i$

TABLE IV: Comparison of QNMs of Schwarzschild black hole for $n = 2$ and $n = 3$ cases (with $M = 1$)

l	QNMs via FNNM $\omega(n = 2)$	$\omega(n = 2)$ [22]	QNMs via FNNM $\omega(n = 3)$	$\omega(n = 3)$ [22]
1	$0.205651 - 0.501614i$	$0.20012 - 0.50331i$	$0.186568 - 0.713255i$	$0.18676 - 0.71153i$
2	$0.405901 - 0.495647i$	$0.40232 - 0.49586i$	$0.361712 - 0.706522i$	$0.36050 - 0.70564i$
3	$0.615296 - 0.489694i$	$0.61511 - 0.49006i$	$0.58184 - 0.692479i$	$0.58141 - 0.69555i$
4	$0.816590 - 0.485938i$	$0.81956 - 0.48700i$	$0.788583 - 0.687117i$	$0.79094 - 0.68923i$
5	$1.0173681 - 0.480342i$	$1.01997 - 0.48525i$	$0.994289 - 0.685727i$	$0.99513 - 0.68511i$

V. CONCLUSIONS

In this paper, we have proposed a new method, FNNM, to study the QNMs of black holes and wormholes. To test the method, we have considered the Schwarzschild black hole and the DSW. Scalar field perturbations have been treated as oscillations in the frequency domain of those static and symmetric backgrounds. The perturbed scalar fields are reduced to a one-dimensional Schrödinger like wave equation. Imposing the required boundary conditions for having the QNMs, we have demonstrated how the FNNM derives the QNMs: Eq. (4.15). After comparing our findings with the previous results obtained by the Mashhoon method (3.7) [33] and Abdalla and Giugno's numerical works [22], it is seen that the all results are in good agreement with each other. Therefore, FNNM is not only an alternative but an effective way for computing the QNMs, which are significant for the question

of the stability of a black hole/wormhole as well as for the late-time behavior of radiation from gravitationally collapsing configurations.

Further work to determine the QNMs of rotating and/or higher/lower dimensional black holes/wormholes via the FNNM could therefore be very interesting. Besides, we aim to extend our analysis to the Dirac and Maxwell equations that are formulated in the Newman-Penrose formalism [77–79]. In this way, we also plan to analyze the quantization [80–84] of spacetimes using the QNMs.

Acknowledgments

This work was supported by Comisión Nacional de Ciencias y Tecnología of Chile through FONDECYT Grant N° 3170035 (A. Ö.).

-
- [1] B. F. Schutz and C. M. Will, “Black Hole Normal Modes: A Semianalytic Approach,” *Astrophys. J.* **291**, L33 (1985).
 - [2] E. Berti, V. Cardoso and A. O. Starinets, “Quasinormal modes of black holes and black branes,” *Class. Quant. Grav.* **26**, 163001 (2009).
 - [3] J. W. Guinn, C. M. Will, Y. Kojima and B. F. Schutz, “High Overtone Normal Modes of Schwarzschild Black Holes,” *Class. Quant. Grav.* **7**, L47 (1990).
 - [4] R. A. Konoplya and A. Zhidenko, “Quasinormal modes of black holes: From astrophysics to string theory,” *Rev. Mod. Phys.* **83**, 793 (2011)
 - [5] S. Iyer, “Black Hole Normal Modes: A Wkb Approach. 2. Schwarzschild Black Holes,” *Phys. Rev. D* **35**, 3632 (1987).
 - [6] K. H. C. Castello-Branco, R. A. Konoplya and A. Zhidenko, “High overtones of Dirac perturbations of a Schwarzschild black hole and the area spectrum of quantum black holes,” *Braz. J. Phys.* **35**, 1149 (2005).
 - [7] K. H. C. Castello-Branco, R. A. Konoplya and A. Zhidenko, “High overtones of Dirac perturbations of a Schwarzschild black hole,” *Phys. Rev. D* **71**, 047502 (2005)
 - [8] J. I. Jing, “Dirac quasinormal modes of Schwarzschild black hole,” *Phys. Rev. D* **71**, 124006 (2005)
 - [9] J. Skakala and M. Visser, “Semi-analytic results for quasi-normal frequencies,” *JHEP* **1008**, 061 (2010).
 - [10] I. Sakalli, “Quasinormal modes of charged dilaton black holes and their entropy spectra,” *Mod. Phys. Lett. A* **28** (2013) 1350109.
 - [11] I. Sakalli, “Quantization of higher-dimensional linear dilaton black hole area/entropy from quasinormal modes,” *Int. J. Mod. Phys. A* **26** (2011) 2263.
 - [12] I. Sakalli, K. Jusufi and A. Övgün, “Analytical Solutions

- in a Cosmic String Born-Infeld-dilaton Black Hole Geometry: Quasinormal Modes and Quantization,” *Gen. Rel. Grav.* **50**, no. 10, 125 (2018).
- [13] A. Övgün and K. Jusufi, “Quasinormal Modes and Greybody Factors of $f(R)$ gravity minimally coupled to a cloud of strings in 2 + 1 Dimensions,” *Annals Phys.* **395**, 138 (2018).
- [14] P. A. Gonzalez, A. Övgün, J. Saavedra and Y. Vasquez, “Hawking radiation and propagation of massive charged scalar field on a three-dimensional Gödel black hole,” *Gen. Rel. Grav.* **50**, no. 6, 62 (2018).
- [15] K. Jusufi, I. Sakalli and A. Övgün, “Quantum tunneling and quasinormal modes in the spacetime of the Alcubierre warp drive,” *Gen. Rel. Grav.* **50**, no. 1, 10 (2018).
- [16] A. Övgün, I. Sakalli and J. Saavedra, “Quasinormal Modes of a Schwarzschild Black Hole Immersed in an Electromagnetic Universe,” *Chin. Phys. C* **42**, no. 10, 105102 (2018).
- [17] J. Crisostomo, S. Lepe and J. Saavedra, “Quasinormal modes of extremal BTZ black hole,” *Class. Quant. Grav.* **21**, 2801 (2004).
- [18] S. Lepe and J. Saavedra, “Quasinormal modes, superradiance and area spectrum for 2+1 acoustic black holes,” *Phys. Lett. B* **617**, 174 (2005).
- [19] J. Saavedra, “Quasinormal modes of Unruh’s acoustic black hole,” *Mod. Phys. Lett. A* **21**, 1601 (2006).
- [20] R. Becar, S. Lepe and J. Saavedra, “Quasinormal modes and stability criterion of dilatonic black hole in 1+1 and 4+1 dimensions,” *Phys. Rev. D* **75**, 084021 (2007).
- [21] R. Becar, S. Lepe and J. Saavedra, “Decay of Dirac fields in the backgrounds of dilatonic black holes,” *Int. J. Mod. Phys. A* **25**, 1713 (2010).
- [22] E. Abdalla and D. Giugno, “An Extensive search for overtones in Schwarzschild black holes,” *Braz. J. Phys.* **37**, 450 (2007)
- [23] M. Casals and A. C. Ottewill, “Spectroscopy of the Schwarzschild Black Hole at Arbitrary Frequencies,” *Phys. Rev. Lett.* **109**, 111101 (2012).
- [24] R. A. Konoplya, “Massive vector field perturbations in the Schwarzschild background: Stability and unusual quasinormal spectrum,” *Phys. Rev. D* **73**, 024009 (2006).
- [25] R. A. Konoplya and C. Molina, “The Ringing wormholes,” *Phys. Rev. D* **71**, 124009 (2005).
- [26] S. W. Kim, “Wormhole perturbation and its quasi normal modes,” *Prog. Theor. Phys. Suppl.* **172**, 21 (2008).
- [27] R. A. Konoplya and A. Zhidenko, “Wormholes versus black holes: quasinormal ringing at early and late times,” *JCAP* **1612**, no. 12, 043 (2016).
- [28] R. Oliveira, D. M. Dantas, V. Santos and C. A. S. Almeida, “Quasi-normal modes of bumblebee wormhole,” arXiv:1812.01798 [gr-qc].
- [29] J. Y. Kim, C. O. Lee and M. I. Park, “Quasi-Normal Modes of a Natural AdS Wormhole in Einstein-Born-Infeld Gravity,” *Eur. Phys. J. C* **78**, no. 12, 990 (2018).
- [30] K. A. Bronnikov, R. A. Konoplya and A. Zhidenko, “Instabilities of wormholes and regular black holes supported by a phantom scalar field,” *Phys. Rev. D* **86**, 024028 (2012).
- [31] S. Aneesh, S. Bose and S. Kar, “Gravitational waves from quasinormal modes of a class of Lorentzian wormholes,” *Phys. Rev. D* **97**, no. 12, 124004 (2018).
- [32] R. A. Konoplya and A. Zhidenko, “Passage of radiation through wormholes of arbitrary shape,” *Phys. Rev. D* **81**, 124036 (2010)
- [33] P. Bueno, P. A. Cano, F. Goelen, T. Hertog and B. Verhocke, “Echoes of Kerr-like wormholes,” *Phys. Rev. D* **97**, no. 2, 024040 (2018).
- [34] S. H. Volkel and K. D. Kokkotas, “Wormhole Potentials and Throats from Quasi-Normal Modes,” *Class. Quant. Grav.* **35**, no. 10, 105018 (2018)
- [35] A. Einstein and N. Rosen, “The Particle Problem in the General Theory of Relativity,” *Phys. Rev.* **48**, 73 (1935).
- [36] C. W. Misner and J. A. Wheeler, Classical physics as geometry, *Ann. Phys.* **2**, 525(1957).
- [37] H. Ellis, Ether flow through a drainhole: A particle model in general relativity, *J. Math. Phys.* **14**, 104 (1973).
- [38] M. S. Morris and K. S. Thorne, “Wormholes in spacetime and their use for interstellar travel: A tool for teaching general relativity,” *Am. J. Phys.* **56**, 395 (1988).
- [39] M. S. Morris, K. S. Thorne and U. Yurtsever, Wormholes, time machines and the weak energy condition, *Phys. Rev. Letts.* **61**, 1446 (1988).
- [40] V. P. Frolov and I. D. Novikov, Physical effects in wormholes and time machines, *Phys. Rev. D* **42**, 1057 (1990).
- [41] E. I. Guendelman, “Wormholes and the construction of compactified phases,” *Gen. Rel. Grav.* **23**, 1415 (1991).
- [42] M. Visser, Lorentzian wormholes: from Einstein to Hawking, AIP Series in Computational and Applied Mathematical Physics, 1996, and references therein.
- [43] J. P. S. Lemos, F. S. N. Lobo and S. Quinet de Oliveira, “Morris-Thorne wormholes with a cosmological constant,” *Phys. Rev. D* **68**, 064004 (2003)
- [44] T. Damour and S. N. Solodukhin, “Wormholes as black hole foils,” *Phys. Rev. D* **76**, 024016 (2007)
- [45] E. I. Guendelman, A. Kaganovich, E. Nissimov and S. Pacheva, “Spherically Symmetric and Rotating Wormholes Produced by Lightlike Branes,” *Int. J. Mod. Phys. A* **25**, 1405 (2010).
- [46] E. I. Guendelman, A. Kaganovich, E. Nissimov and S. Pacheva, “Einstein-Rosen ‘Bridge’ Needs Lightlike Brane Source,” *Phys. Lett. B* **681**, 457 (2009).
- [47] E. Teo, “Rotating traversable wormholes,” *Phys. Rev. D* **58**, 024014 (1998)
- [48] K. A. Bronnikov and J. P. S. Lemos, “Cylindrical wormholes,” *Phys. Rev. D* **79**, 104019 (2009).
- [49] I. Sakalli and A. Ovgun, “Tunnelling of vector particles from Lorentzian wormholes in 3+1 dimensions,” *Eur. Phys. J. Plus* **130**, no. 6, 110 (2015).
- [50] G. Clement, “Wormhole cosmic strings,” *Phys. Rev. D* **51**, 6803 (1995).
- [51] G. T. Horowitz, D. Marolf, J. E. Santos and D. Wang, “Creating a Traversable Wormhole,” arXiv:1904.02187 [hep-th].
- [52] J. Maldacena, A. Milekhin and F. Popov, “Traversable wormholes in four dimensions,” arXiv:1807.04726 [hep-th].
- [53] P. Gao, D. L. Jafferis and A. Wall, “Traversable Wormholes via a Double Trace Deformation,” *JHEP* **1712**, 151 (2017).
- [54] I. Sakalli and A. Ovgun, “Gravitinos Tunneling From Traversable Lorentzian Wormholes,” *Astrophys. Space Sci.* **359**, no. 1, 32 (2015).
- [55] A. Ovgun and M. Halilsoy, “Existence of traversable wormholes in the spherical stellar systems,” *Astrophys. Space Sci.* **361**, no. 7, 214 (2016).
- [56] A. Ovgun, “Rotating Thin-Shell Wormhole,” *Eur. Phys. J. Plus* **131**, no. 11, 389 (2016).

- [57] K. Jusufi, A. Övgün and A. Banerjee, “Light deflection by charged wormholes in Einstein-Maxwell-dilaton theory,” *Phys. Rev. D* **96**, no. 8, 084036 (2017).
- [58] M. Halilsoy, A. Ovgun and S. H. Mazharimousavi, “Thin-shell wormholes from the regular Hayward black hole,” *Eur. Phys. J. C* **74**, 2796 (2014).
- [59] K. Jusufi and A. Övgün, “Gravitational Lensing by Rotating Wormholes,” *Phys. Rev. D* **97**, no. 2, 024042 (2018).
- [60] M. G. Richarte, I. G. Salako, J. P. Morais Graa, H. Moradpour and A. Övgün, “Relativistic Bose-Einstein condensates thin-shell wormholes,” *Phys. Rev. D* **96**, no. 8, 084022 (2017).
- [61] A. Övgün, “Light deflection by Damour-Solodukhin wormholes and Gauss-Bonnet theorem,” *Phys. Rev. D* **98**, no. 4, 044033 (2018).
- [62] A. Abdujabbarov, B. Juraev, B. Ahmedov and Z. Stuchlik, “Shadow of rotating wormhole in plasma environment,” *Astrophys. Space Sci.* **361**, no. 7, 226 (2016).
- [63] G. Gyulchev, P. Nedkova, V. Tinchev and S. Yazadjiev, “On the shadow of rotating traversable wormholes,” *Eur. Phys. J. C* **78**, no. 7, 544 (2018).
- [64] K. Akiyama *et al.* [Event Horizon Telescope Collaboration], “First M87 Event Horizon Telescope Results. I. The Shadow of the Supermassive Black Hole,” *Astrophys. J.* **875**, no. 1, L1 (2019).
- [65] R. A. Konoplya, “How to tell the shape of a wormhole by its quasinormal modes,” *Phys. Lett. B* **784**, 43 (2018) *Eur. Phys. J. C* **78**, no. 12, 990 (2018).
- [66] B. Mehlig, *Artificial Neural Networks* (2019). arXiv:1901.05639
- [67] D. R. Parisi, M. C. Mariani, M. A. Laborde, “Solving differential equations with unsupervised neural networks,” *Chem. Eng. Process.* **42**, 715-721 (2003)
- [68] N. Yadav, A. Yadav, M. Kumar, “An Introduction to Neural Network Methods for Differential Equations,” Springer, (2015).
- [69] H. Mutuk, “Cornell Potential: A Neural Network Approach,” *Adv. High Energy Phys.* **2019**, 3105373 (2019).
- [70] H. Mutuk, “Mass Spectrum of Exotic X(5568) State via Artificial Neural Network,” arXiv:1901.01154 [hep-ph].
- [71] H. Nakano *et al.*, “Comparison of various methods to extract ringdown frequency from gravitational wave data,” arXiv:1811.06443 [gr-qc].
- [72] V. Ferrari and B. Mashhoon, “New approach to the quasinormal modes of a black hole,” *Phys. Rev. D* **30**, 295 (1984).
- [73] S. Chakraverty, S. Mall, *Artificial Neural Networks for Engineers and Scientists-Solving Ordinary Differential Equations*, CRC Press, 2017.
- [74] I. E. Lagaris, A. Likas and D. I. Fotiadis, “Artificial neural network methods in quantum mechanics,” *Comput. Phys. Commun.* **104**, 1 (1997).
- [75] A. Liaqat, M. Fukuhara, and T. Takeda, *Computer Physics Communications* **141**, 350 (2001).
- [76] D.-P. Du, B. Wang, and R.-K. Su, *Physical Review D* **70**, (2004).
- [77] E. Newman and R. Penrose, “An Approach to gravitational radiation by a method of spin coefficients,” *J. Math. Phys.* **3**, 566 (1962).
- [78] S. Chandrasekhar, *The Mathematical Theory of Black Holes* (Oxford University Press, Oxford, 1983).
- [79] I. Sakalli and M. Halilsoy, “Solution of Dirac equation in the near horizon geometry of an extreme Kerr black hole,” *Phys. Rev. D* **69**, 124012 (2004).
- [80] J. D. Bekenstein, “The quantum mass spectrum of the Kerr black hole,” *Lett. Nuovo Cim.* **11**, 467 (1974).
- [81] J. D. Bekenstein, “Quantum black holes as atoms,” gr-qc/9710076.
- [82] J. D. Bekenstein, “Black holes: Classical properties, thermodynamics and heuristic quantization,” gr-qc/9808028.
- [83] I. Sakalli, “Quantization of rotating linear dilaton black holes,” *Eur. Phys. J. C* **75**, no. 4, 144 (2015)
- [84] I. Sakalli and G. Tokgoz, “Spectroscopy of rotating linear dilaton black holes from boxed quasinormal modes,” *Annalen Phys.* **528**, 612 (2016).